The Canadian Mineralogist
Vol. 34, pp. 37-48 (1996)

MICRO-PIXE ANALYSIS OF SILICATE REFERENCE STANDARDS FOR TRACE Ni, Cu, Zn, Ga, Ge, As, Rb, Sr, Y, Zr, Nb, Mo AND Pb, WITH EMPHASIS ON Ni FOR APPLICATION OF THE Ni-IN-GARNET GEOTHERMOMETER*

JOHN L. CAMPBELL AND WILLIAM J. TEESDALE

Guelph–Waterloo Program for Graduate Work in Physics, University of Guelph, Guelph, Ontario N1G 2W1

BRUCE A. KJARSGAARD

Geological Survey of Canada, 601 Booth Street, Ottawa, Ontario K1A OE8

LOUIS J. CABRI

CANMET, 555 Booth Street, Ottawa, Ontario K1A OG1

ABSTRACT

Trace-element analysis is a powerful tool for studying numerous processes of research interest in the Earth Sciences; as well, it has important applications of interest to the mineral exploration community. Here, we present the results of a comprehensive study of five internationally recognized silicate reference standards (BHVO–1, GXR–5, GSR–5, MAG–1 and GSD–50) utilizing micro-PIXE analysis. Results of trace analyses for Ni, Cu, Zn, Ga, Ge, As, Rb, Sr, Y, Zr, Nb, Mo and Pb are presented. Measured data for the five standards exhibit agreement within ±10%, and commonly better, with recommended levels of concentration in the 50–400 ppm range. Detection limits (for a typical 3- to 4-minute analysis of an accumulated charge of 2.5 microCoulombs) are in the range of 2–10 ppm, with precisions of 1–10%. A detailed study of the X-ray spectra in the vicinity of the Fe, Ni and Co lines illustrates that the GUPIX software is able to correctly fit the complex spectra and thus provide accurate Ni concentrations. Further tests on Ni in garnet are reported, in the context of current application of the Ni-in-garnet geothermometer in diamond exploration; it appears important to resolve the difference between the two published calibrations of this important geothermometer.

Keywords: micro-PIXE analysis, geostandards, trace elements, acccuracy, glasses, garnet, Ni-in-garnet geothermometer.

SOMMAIRE

L'analyse chimique de matériaux pour leur teneur en éléments traces constitue un outil puissant dans l'étude des nombreux processus géologiques, et ses applications dans les programmes d'exploration minière sont importantes. Nous présentons ici les résultats d'une étude intégrée de cinq étalons de silicate à circulation internationale (BHVO–1, GXR–5, GSR–5, MAG–1 et GSD–50) utilisant la méthode micro-PIXE. Nous présentons les résultats d'analyses pour le Ni, Cu, Zn, Ga, Ge, As, Rb, Sr, Y, Zr, Nb, Mo et Pb. Les concentrations mesurées concordent à 10% près, et dans plusieurs cas, à moins que 10% près, avec les concentrations recommandées, dans l'intervalle 50–400 ppm. Le seuil de détection, pour le cas d'une analyse typique, d'une durée de 3 à 4 minutes et ayant une charge accumulée de 2.5 microCoulombs, est entre 2 et 10 ppm, avec une précision d'entre 1 et 10%. Une étude détaillée des spectres de rayons X dans la région des raies Fe, Ni et Co montre que le logiciel GUPIX peut reproduire correctement la complexité des spectres, et ainsi mener à une détermination précise de la concentration du Ni. Nous présentons les résultats d'une évaluation de la teneur en Ni d'échantillons de grenat, dans le contexte du géothermomètre fondé sur cet élément, et de ses applications à l'exploration pour le diamant. Il semble maintenant essentiel de résoudre les différences entre les deux calibrages de ce géothermomètre important déjà dans la littérature.

(Traduit par la Rédaction)

Mots-clés: analyse micro-PIXE, étalons, éléments traces, justesse, verres, grenat, géothermométrie.

---

* Geological Survey of Canada contribution number 24795.

INTRODUCTION

Microbeam trace-element techniques are well suited for analysis of minerals and glasses (or their microcrystalline equivalents). In this respect, micro-PIXE, a non-destructive technique, allows specimens to be studied using both electron and proton microprobe analysis for major, minor and trace elements. Applications of the data include studies of solid–liquid and liquid–liquid partition coefficients for petrogenetic trace-element modeling of magmatic processes (for an up-to-date review, see Foley & van der Laan 1994). Micro-PIXE analysis of experimental run-products to determine trace-element partitioning includes the work of Sweeney *et al.* (1992), Adam *et al.* (1993) and Vicenzi *et al.* (1994). Micro-PIXE mineral–melt partitioning studies have also been undertaken in glassy volcanic rocks (*e.g.*, Stimac & Hickmott 1994, Ewart & Green 1994). Another main use of micro-PIXE is to characterize trace-element signatures of mineral phases from specific types of magmatic or ore-forming fluid systems. Relevant micro-PIXE studies on apatite, zircon, titanite, carbonates and sulfides are reviewed by Halden *et al.* (1995). Important micro-PIXE studies have also been undertaken on a variety of mantle phases (*e.g.*, olivine, garnet, spinel, clinopyroxene and orthopyroxene) for characterization of trace-element concentration (Moore *et al.* 1992, Griffin *et al.* 1989). Applications of this work include the garnet/olivine Ni-exchange thermometer (Griffin *et al.* 1989, Griffin & Ryan 1995), utilized for studies of diamond exploration and associated mantle petrology (*e.g.*, the conditions of diamond formation).

BACKGROUND INFORMATION

The partitioning of nickel between chromian pyrope (garnet) and olivine in kimberlite- or lamproite-derived mantle xenoliths exhibits a well-defined dependence on temperature of equilibration. The relative variation of nickel content among grains of garnet in such xenoliths is very much greater than that in olivine. Griffin *et al.* (1989) and Griffin & Ryan (1995) determined the Ni content of garnet grains *in situ* by the micro-PIXE technique (Campbell *et al.* 1989, Ryan *et al.* 1990). This approach involves the recording in energy-dispersion mode of the X-ray spectrum emitted under bombardment by a 3-MeV beam of protons. Micro-PIXE is well suited to this application because its low detection-limit for nickel. A 5-minute measurement using some 10 nA of current focused in a 20 × 20 μm spot leads to a detection limit of about 5 ppm. For comparison, the concentration range is 0–150 ppm in the grains of interest. The work of Griffin *et al.* (1989) and Griffin & Ryan (1995) has resulted in the development of an empirical geothermometer. By assuming a constant nickel content of 2900 ppm in mantle olivine, the "nickel thermometer" provides an estimate of equilibration temperature solely on the basis of measured nickel concentration in garnet grains derived from the kimberlite or lamproite host. Although the precise calibration of the thermometer is being challenged (*cf.* Canil 1994, Griffin & Ryan 1995), the nickel thermometer is a powerful addition to the array of tools available to evaluate the diamond potential of garnet-bearing igneous formations. Furthermore, additional trace-element data (*e.g.*, Y, Zr, Sr, Ga) obtained by PIXE analysis of garnet provide chemical signatures inferred to be related to specific processes in the mantle (*e.g.*, metasomatism) which can affect the likelihood of diamond preservation.

There are only a small number of micro-PIXE facilities suitable for the analysis of mineral specimens around the world, and only a subset of these have developed experience in the quantitative analysis of mineral grains. There is, as yet, only a modest quantity of documentation of the results of micro-PIXE analysis of internationally recognized geochemical reference standards. Ryan *et al.* (1990) and Czamanske *et al.* (1993) have analyzed well-characterized silicate glasses, including a number of fused geological standard reference materials.

The determination of trace concentrations of Ni in silicates, however, presents a special challenge. As the PIXE spectrum of BHVO–1 basaltic glass in Figure 1 demonstrates, the very weak Ni$K\alpha$ X-ray line lies on the flank of the very intense Fe$K\beta$ line. The intensity ratio of about 100:1 reflects the typical concentrations of several percent for Fe and several tens of ppm for Ni associated with chromian pyrope. Even a small error in the fitting of the Fe lines in the spectrum or of the underlying continuum background could cause significant error in the inferred concentration of Ni, which has important implications for Ni thermometry.

The first purpose of this study is to test the accuracy of micro-PIXE analysis of five reference standards for ten trace elements commonly used in petrogenetic modeling. Our second purpose is to test our micro-PIXE methodology for the specific case of Ni across the range of concentrations germane to Ni thermometry of garnet.

METHODS

Sample description and preparation

Five geochemical reference materials were employed. These comprised the USGS materials MAG–1 (marine mud), GXR–5 (shale) and BHVO–1 (basalt), the Chinese material GSR–5 (soil), and the artificial glass GSD–50. Two of the present authors participated in the micro-PIXE analysis of BHVO–1 by Czamanske *et al.* (1993), but a re-analysis was considered justified by various minor improvements effected since in our methodology. Samples of the first

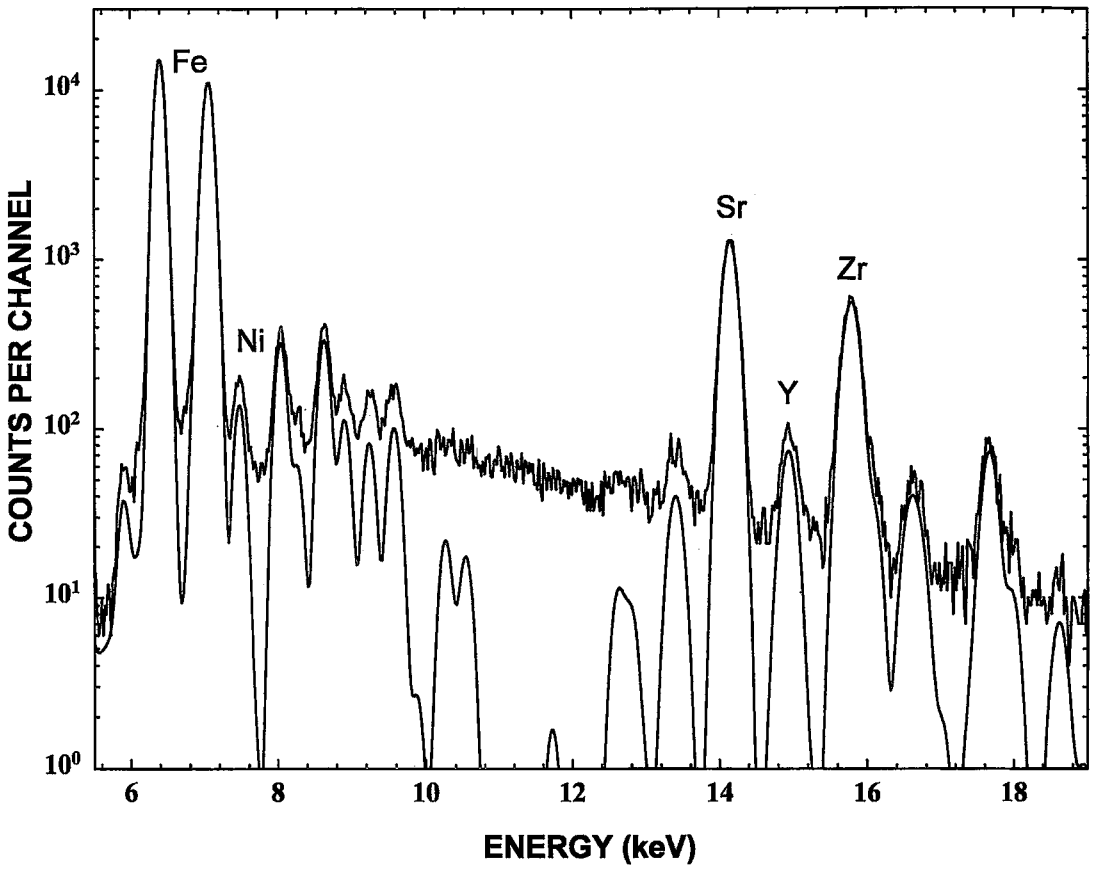

FIG. 1. Micro-PIXE spectrum of a silicate glass containing approximately 120 ppm nickel, fitted as described in the text.

three materials were prepared by fusion on an iridium strip heater; in each case, three 0.25-g samples of powder were individually fused. The three resulting glasses were then ground together in an agate mortar, and from this material, 0.25 g was removed and fused. The 0.25 g product of the second fusion was reground and refused. Each fusion was done in air at a temperature 400°C below the melting point of iridium, and lasted some 3–4 minutes. The pieces of glass chosen for micro-PIXE analysis were taken from the region furthest from the face that was in contact with the iridium strip, in order to minimize possible contamination by iridium or by trace metals in the strip. Details of the fusion of the USGS BHVO–1 basalt material have been published by Czamanske *et al.* (1993). The artificial glass GSD–50 is one of a set of standards prepared by the Corning Glass Works for the U.S. Geological Survey (Myers *et al.* 1976). Portions of each glass were mounted in epoxy blocks, polished, and carbon-coated to provide a conducting path for the beam of charged particles.

The practice adopted by Gladney & Roelandts (1988, 1990) to generate recommended concentrations for geological reference materials is an iterative one. The first step is to calculate, for a given trace element in a given material, the mean and standard deviation of all available published concentrations derived from a selected set of analytical techniques. Any values that depart from the mean by more than two standard deviations are then rejected, following which the mean and standard deviation are recomputed. The values recommended by Myers *et al.* for the GSD–50 glass were arrived at in a different manner. We have therefore subjected the raw data of Myers *et al.* to the procedure of Gladney & Roelandts in order to provide recommended concentrations; in doing so, we have restricted ourselves to data listed by Myers *et al.* as "quantitative" and have excluded "semi-quantitative" data. In the case of GSR–5, Xie *et al.* (1989) provided only a recommended concentration with no attached uncertainty; we have therefore again used the approach of Gladney & Roelandts to provide values of concen-

tration and uncertainty consistent with those of the other standards used here.

Micro-PIXE analysis

Micro-PIXE analysis was conducted at the Guelph Scanning Proton Microprobe, using a 12 nA beam of 3 MeV protons; the spot size was typically 15 μm^2. An Oxford Instruments Si(Li) detector of approximately 80 mm^2 area located 25 mm from the specimen provided the most efficient possible geometry. The detector's energy resolution, expressed in the conventional manner as the full-width at half height of the Mn$K\alpha$ line, was 145 eV. The 125 μm Mylar absorber normally used to suppress low-energy bremsstrahlung background was supplemented by an aluminum absorber (nominal thickness 250 μm) whose function was to reduce the iron contribution to the X-ray spectrum and thereby permit better statistics to be amassed for the trace element peaks than would otherwise be the case.

Spectra were recorded at ten spots on each specimen except for BHVO–1, in which case five spots were studied. The accumulated proton charge for each spectrum was 2.5 microCoulombs, and the time taken was typically between 3 and 4 minutes.

Full details of the use of the NIST standard reference material SRM 1155 (a molybdenum steel alloy) to calibrate the system are given by Campbell *et al.* (1993) and by Czamanske *et al.* (1993). The essence of the approach is that the 2.38% Mo in the SRM determines the instrumental constant for our system, and the 64.5% iron gives a very accurate determination of the thickness of the aluminum absorber.

Data reduction

Data were processed using the GUPIX software package developed at Guelph for PIXE analysis (Maxwell *et al.* 1989, 1995). The process involves two main steps. First, a model spectrum is fitted to the measured spectrum to ascertain the peak areas. Then these areas are converted to element concentrations using the measured instrumental constant, the known characteristics of the detector and the absorber, and matrix corrections that account for the role of the major elements in slowing down the incident protons and attenuating the emitted X-rays. In order to compute these matrix corrections, GUPIX requires, in addition to its database, the major-element concentrations in the specimens; these were taken from the literature (Myers *et al.* 1976, Govindaraju 1989, Xie *et al.* 1989, Gladney & Roelandts 1988, 1990).

It is in the treatment of the energy-dispersed X-ray spectrum that approaches within the PIXE community tend to differ. Most codes build the model spectrum using Gaussian peaks superposed on a continuum background; in some cases, an analytical expression (*e.g.*, a high-order exponential polynomial) is used as background model, whereas in others, a peak-removal algorithm is used to generate the background, which is subsequently employed in numerical form as part of the model. The model spectrum is then matched to the measured one by nonlinear least-squares fitting, using chi-squared as the goodness-of-fit criterion.

GUPIX differs from the majority of codes in its treatment of continuum background. Its approach is based on the properties of the simple digital filter, shown in Figure 2, along with its effect upon a very simple spectrum. This "top hat" filter method is widely

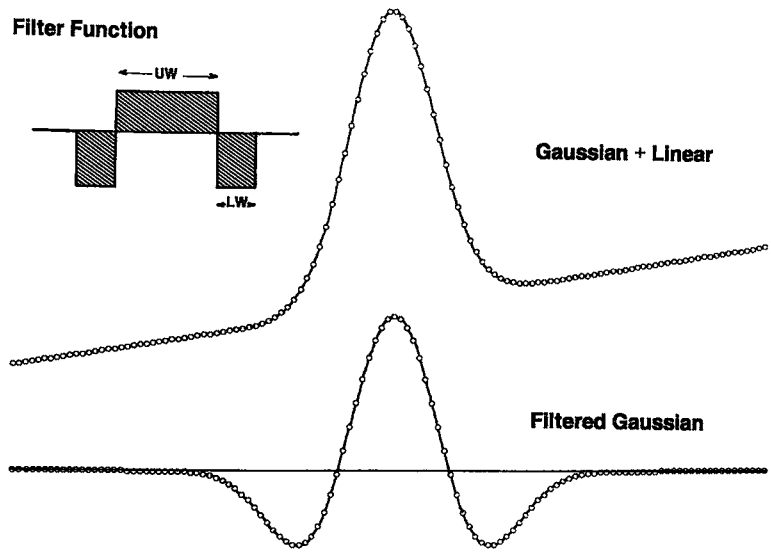

FIG. 2. The "top hat" digital filter used to suppress background, together with its effect upon a simple spectrum.

used in the treatment of electron microprobe X-ray spectra (McCarthy & Schamber 1981); its effect is to suppress linear background entirely and to modify Gaussian peak shapes. It will be an effective remover of background over an entire spectrum provided that the continuum is locally close to being linear over any region of width equivalent to the filter width; the latter is chosen to equal one full-width at half-height at the spectrum center.

The intense peaks due to major elements such as iron exhibit significant low-energy tailing. The peak model in GUPIX includes quasi-exponential features to describe these, but in the large-area detector that is necessary for trace-element analysis, their intensity is observed to change over a single day of measurement. Such changes are reported also by other PIXE investigators (Larsson *et al.* 1989, Ryan *et al.* 1990). One way to deal in general with the rather poorly known tailing features, and in particular with their time-dependence, is to de-emphasize their influence upon the fit. We describe in detail elsewhere (Maxwell *et al.* 1994) a procedure to do this. It augments the conventional statistical error in channel content by an amount that diminishes exponentially from the centroid on the low-energy side of intense peaks, and propagates the augmented error into the channel weights. An alternative is to define, following Benjamin *et al.* (1988), an error in the thickness of the absorbing filter, and to propagate this into the weights; because this error is largest for low-energy peaks of the major elements, it de-emphasizes the influence of the entire iron peaks upon the goodness-of-fit. Although we consider the first approach preferable, we observe that the two methods give concentrations for nickel and other trace elements that differ by less than 1 ppm.

Results

Overall results for thirteen trace elements

Table 1 displays the entire set of results in terms of the mean concentrations over ten spots and the corresponding standard deviations. The ratio (h) of the standard deviation to the error of a single measurement provides a measure of the homogeneity of the distribution of each element in each material analyzed. Table 1 includes the mean-h values obtained by averaging over the trace elements in each specimen. It seems that the fusions achieved good homogeneity. There are two exceptions. In GSR–5, the value of h found for Zr is 5.1, indicating that the fusion had not successfully redistributed the Zr. In GSR–5, GXR–5 and MAG–1, traces of Ir are observed, and its distribution is highly heterogeneous; the Ir is presumably derived from the filament. The results were not included in the calculation of h.

Our results have been corrected for the loss of volatiles (*e.g.*, bound water) during the fusion, and so they may be compared directly with the nominal values, which have been taken from the literature, as indicated in Table 1. The agreement is generally good, with some specific exceptions. In the three materials fused on the iridium strip, the measured concentration of Zr is high by 20 – 140%, suggestive of Zr contamination in the glass. This may be contrasted to the cases of BHVO–1 and GSD–50, where the measured and nominal results are in good agreement. In MAG–1, the measured concentration of Zn is low by a factor of three, and the measured concentration of Sr is high by 25%; we have no explanation for these two anomalies in MAG–1. Ge, Mo and Pb were detected only in

TABLE 1. MEASURED (M) AND NOMINAL (N) CONCENTRATIONS OF THIRTEEN TRACE ELEMENTS*

	GXR-5		GSR-5		MAG-1		BHVO-1		GSD-50	
	M	N[1]	M	N[2]	M	N[3]	M	N[3]	M	N[4]
Ni	75±4	75±8	36±5	37±?	40±4	53±8	119±6	121±2	46±5	54±7
Cu	335±18	354±34	50±3	42±3	26±2	30±3	160±3	136±?	42±3	46±7
Zn	32±3	49±9	53±4	55±6	38±3	130±6	113±3	105±5	42±2	41±6
Ga	47±4	40±4	28±2	25.6±3.4	24±2	20.4±1.5	22±2	21±2	3±1	—
Ge	nd[5]		nd		nd		nd		35±2	37±5
As	4±2	11±2	4±2	1.4±0.4	8±2	9.2±1.2	nd	0.4±?	34±2	—
Rb	39±2	41±3	212±4	205±12	139±4	149±6	9±1	11±2	33±2	41±4
Sr	119±2	110±8	120±3	90±11	205±5	146±15	398±3	403±?	64±3	64±7
Y	16.5±1.5	16±1.5	26±3	26±3	25±2	28±3	23.5±0.5	27.6±17	38±1	46±4
Zr	218±4	140±40	240±20	96±13	155±6	126±13	170±3	179±21	41±2	46±3
Nb	7.6±1.7	6.7±2.6	13±2	14.3±2.5	14.5±2	12±2	18±1	19±2	41±3	42±2
Mo	nd		nd		nd		nd		33±2	46±3
Pb	nd		nd		nd		nd		51±3	52±5
h	1.0		1.5(1.1)[6]		0.9		1.0		0.8	

* Measured values are mean and standard deviation for 10 spots. Nominal values are recommended concentration and standard deviation.

[1] Gladney & Roelandts (1990); [2] Xie *et al.* (1989); [3] Gladney & Roelandts (1988); [4] Myers *et al.* (1976); [5] nd: not detected; [6] Zr omitted.

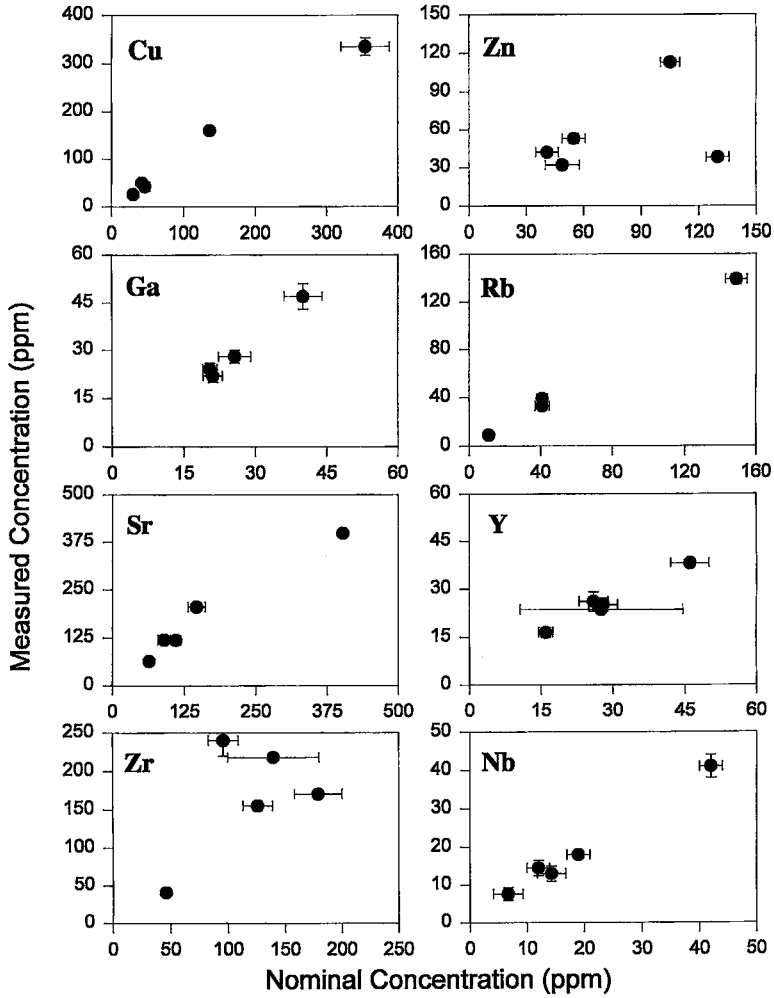

FIG. 3. Graphical comparison of measured and recommended concentrations of Cu, Zn, Ga, Rb, Sr, Y, Zr, Nb in five geochemical reference materials.

GSD–50, where good agreement with nominal concentrations was observed. The results for Cu, Zn, Ga, Rb, Sr, Y, Zr, Nb are summarized graphically in Figure 3, and those for Ni are discussed separately below.

Results for nickel

Results for Ni are summarized in Table 2, again in terms of the mean concentrations and the standard deviations from ten spots. The result for Ni is influenced by whether or not the neighboring element cobalt is included in the list of elements whose X-ray lines are to comprise the model spectrum. This influence arises because the Co*K*β line is very close in

TABLE 2. DEPENDENCE OF MEASURED CONCENTRATIONS OF NICKEL (ppm) ON THE MANNER OF FITTING COBALT*

Fit		GXR-5	GSR-5	MAG-1	BHVO-1	GSD-50
	Fe(%)	3.75	5.68	5.66	8.64	4.9
	Ni/Fe[b]	20	6.5	9.4	14	11
A	Ni	82.5±3.7	39.2±4.0	42.2±4.1	123.5±5.6	47.7 ±4.7
	Co	37±13	13±10	7±12	31±19	0.0
B	Ni	76.4±5.1	37.3±4.8	41.3±4.3	118.7±6.8	47.6±4.6
C	Ni	76.2±4.1	35.9±4.8	40.4±4.1	118.7±5.6	45.7±4.6
	Co	6±6	11±11	3±8	16±15	0.0
Nominal	Ni	75±8	37±3	53±8	121±2	55±6
Nominal	Co	29.9±1.2	21±2	20.4±1.6	45±2	35.0

*See text for description of fit procedures A, B, C.

[b]Ratio is in units of ppm Ni relative to % Fe.

energy to the Ni$K\alpha$ line. The nominal concentration of Co in the five glasses ranges from 21 to 45 ppm. Because the Co$K\alpha$ line is superimposed on the lower flank of the intense Fe$K\beta$ line, the detection limit of Co is very high (180 – 340 ppm). Nonetheless, the fit (referred to as fit A) in some cases reports non-zero concentrations of Co (10–40 ppm). If Co is then omitted from the element list and the fit repeated (B), the observed concentrations of Ni decrease by a few ppm, as shown in Table 2.

These observations, coupled with the low levels of Co in the five reference standards, tend to support the omission of Co routinely in our fits to the PIXE spectra of the fused glasses. However, in the case of chromian pyrope garnet, there is some danger in adopting this as a general assumption. Analysis of mantle garnet for Co has been undertaken in only a few studies. Shimizu & Allègre (1978) determined Co concentration by SIMS in garnet from 14 mantle xenoliths, and reported concentrations in the range 33 – 92 ppm Co. In particular, they reported 50 ppm Co in mantle xenolith PHN1611. Merlet & Boudinier (1990) also studied xenolith PHN1611, and indicated similar concentrations of Co, in the range of 57–75 ppm (as determined by high-precision wavelength-dispersion electron microprobe). Hervig *et al.* (1986) analyzed 31 samples of garnet from a variety of "cold" and "hot" garnet lherzolite xenoliths for Co by SIMS. Co concentrations were found to range from 66 to 127 ppm. They noted that these levels are 10 to 50% higher than those reported by Shimizu & Allègre (1978). Hervig *et al.* (1986) suggested that the difference between the two studies is related to their use of a nonoptimal inter-mineral matrix-correction scheme. It can thus be suggested on the basis of previous work that typical Co concentrations in mantle garnet are in the order of 30–100 ppm.

In micro-PIXE analysis of garnets for Co at these levels of concentration, it is important to assess the influence of the Co$K\beta$ X-ray line on the Ni$K\alpha$ line. We therefore modified our fitting code to treat the Co$K\alpha$ and $K\beta$ lines as representing two separate "elements", *i.e.*, the lines were not constrained in the model spectrum to maintain the intensity ratio quoted in the literature (Maxwell *et al.* 1989). Any concentration reported *via* Co$K\alpha$ can then be ignored, given the high limit of detection. But for Co$K\beta$, the limit of detection is 40 ppm, and so there is the possibility to observe lower concentrations of Co than in the conventional approach. This approach is referred to as C; considering that the typical range of concentration in mantle garnet is 30–100 ppm (close to or greater than the 40 ppm limit of detection), approach C is recommended for the analysis of mantle garnet. In each of the C-type fits to the glass spectra, the concentration of Co is reported at a level below the limit of detection, and the Ni value is slightly lower than in fits A and B. The Ni data reported in Table 1 are those of method C.

The variation in Ni content among the three sets of results gives some crude measure of the systematic uncertainty caused by the proximity of the cobalt and nickel lines.

Discussion

Comparison of micro-PIXE to other microbeam techniques

In common with other analytical techniques [*e.g.*, X-ray fluorescence (XRF), instrumental neutron-activation analysis (INAA), inductively coupled plasma – atomic emission spectroscopy (ICP–AES), inductively coupled plasma – mass spectrometry (ICP–MS)] and microbeam trace-element analytical techniques [*e.g.*, secondary-ion mass spectrometry (SIMS), laser-ablation mass spectrometry with inductively coupled plasma (LAM–ICP–MS), synchrotron X-ray fluorescence (SXRF)], micro-PIXE has its own inherent set of strengths and weaknesses in terms of methodology and application. Recent discussions of microbeam analytical techniques are provided by Reed (1990) and Green (1994). One major strength of micro-PIXE (as compared to SIMS and LAM–ICP–MS) is that it is a nondestructive technique. Furthermore, micro-PIXE is essentially a fundamental-parameter technique that requires a single normalization factor or instrumental constant, which may be determined from a simple few-element standard (*e.g.*, NIST 1155, as described above). In contrast, SIMS instruments are calibrated by utilizing working curves developed from relevant standards. Once standards and working curves are obtained, however, SIMS has the advantage of being able to analyze for a wide range of elements (to ppm detection limits) with good spatial resolution (Green 1994). The LAM–ICP–MS technique is currently at an early stage of development (Green 1994). Instrument calibration utilizes spiked reference standards. Recent work (*e.g.*, Jackson *et al.* 1992, Perkins *et al.* 1993, Fryer *et al.* 1995, Ludden *et al.* 1995, Jeffries *et al.* 1995) illustrate the potential for analysis of glasses and a variety of mineral phases for a number of elements at low levels of detection.

Trace elements (except Ni)

Both the precision and the accuracy of micro-PIXE may be estimated from the data of Table 1. Precision is expressed as the ratio (percentage) of standard deviation to mean measured concentration for the ten measurements on a given element in a given glass. Inspection shows that it is typically 1% for concentrations around 400 ppm, 2–3% for concentrations in the vicinity of 100 ppm, and 5–10% for concentrations around 50 ppm. Because the specimens have a homogeneous distribution of trace elements, the precision is determined mainly by counting statistics, and therefore

if the measurement time is increased by a given factor (at constant beam-current), then the precision will improve as the square root of that factor. We have estimated the accuracy of the determination of concentration for each element by the simple expedient of averaging the percentage difference between measured and nominal concentrations over the five glasses. Two types of data are omitted in this calculation. Concentrations below 10 ppm are omitted because their statistical error introduces too much uncertainty. The few cases of obvious large discrepancies also are omitted: these are Zn in MAG–1, and both Sr and Zr in the three glasses fused on the Ir strip. In the case of Sr, the measured concentrations are on average some 27% high in these three cases, but they differ by less than 1% from nominal concentrations in the remaining two glasses. For the elements Cu, Zn, Ga, Ge, Rb, Sr, Y, Nb and Zr, the average determined by this method is ±10%; only one measurement is available for each of Ge, Mo and Pb, but the 10% estimate holds for the first and third of these.

Analysis for nickel

Figure 4 presents a summary of the results for nickel concentrations. For the standards GSR–5, GXR–5 and BHVO–1, the agreement between measured and nominal concentrations is excellent. The results for MAG–1 and GSD–50 are lower than the expected values, but for the latter, there is overlap between the uncertainty bars of the measured and nominal concentration. It should be noted that the recommended concentrations for GSD–50 are based upon measurements performed prior to 1976; these concentrations are therefore somewhat less well-founded than those of the other reference materials employed here. For completeness, other published PIXE results for Ni in geochemical reference standards are given in Table 3.

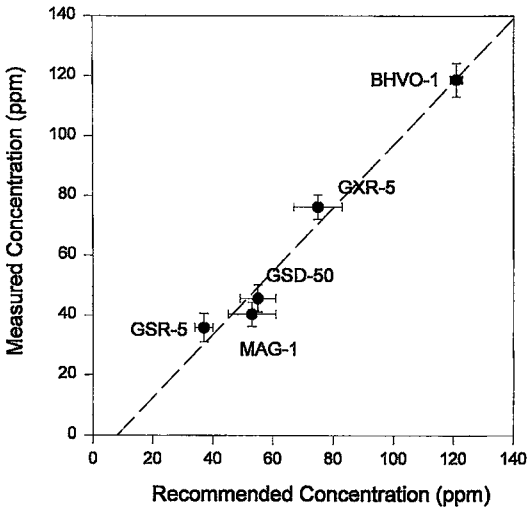

FIG. 4. Graphical comparison of measured and recommended Ni concentrations in geochemical reference materials. The regression is y = –8.2 + 1.053x, with correlation coefficient = 0.988.

TABLE 3. PUBLISHED MICRO-PIXE RESULTS ON NICKEL CONCENTRATIONS IN GEOCHEMICAL REFERENCE MATERIALS

Material	Ni concentration (ppm)		Reference
	Nominal	Measured	
BCR-1	13	13 ± 3	Ryan et al. (1990)
AGV-1	166	15 ± 2	Ryan et al. (1990)
GSP-1	10	6 ± 2	Ryan et al. (1990)
BHVO-1	121	131	Czamanske et al. (1993)
		123	Czamanske et al. (1993)

The micro-PIXE analysis for Ni merits more extensive discussion, partly because of the technical difficulty that is evident in fitting the spectra, and partly because of the importance of the Ni thermometer as a tool in diamond exploration. The Ni results must first be considered in the established context of the overall accuracy for other trace elements; the accuracy figures given in the preceding paragraph suggest that for nickel between 50 and 150 ppm, the accuracy would be in the range 2–10%, the upper value applying to the lower concentrations. However, this argument fails to consider the special problem of overlap with the iron lines that is encountered in the Ni case. The potential for error might be expected to increase as the Ni/Fe concentration ratio (R) decreases. This ratio (in units of ppm Ni/Fe) is therefore included in Table 2. At the highest values of R, encountered in GXR–5 and BHVO–1, measured and nominal Ni concentrations (obtained by method C) agree at the 1–2% level. At the lowest value of R (GSR–5), there is agreement at the 3% level. It is therefore difficult to understand why in the two cases with intermediate R-values (MAG–1 and GSD–50), the measured values are, respectively, 24 and 17% lower than the nominal values. It is worth noting, however, that in GSD–50, the elements Rb, Y and Mo show very similar discrepancies to that for Ni.

Fedorowich *et al.* (1995) have recently published results of a LAM–ICP–MS/micro-PIXE study directly relevant to the present work. Data from this study provide an interesting comparison of the two analytical techniques. A strength of micro-PIXE is the ability to examine certain transition elements, *e.g.*, Ni, Cu, Zn, Ga, Ge, As, Co (as well as Rb and Nb) at low concentrations. In contrast, analysis of these specific elements by LAM–ICP–MS can be problematic for a number of reasons. From a technical standpoint, problems arise during analysis for transition elements by LAM–ICP–MS owing to: (a) high backgrounds caused

by polyatomic compounds of the major plasma constituents of the ICP [Ar, N, O, C, (H)]; (b) interferences by polyatomic ions from the major matrix minerals (*e.g.*, $^{40}Ca^{16}O$ on ^{56}Fe, $^{44}Ca^{16}O$ on ^{60}Ni), (c) differential ablation-behavior than for the lithophile major elements commonly used as internal standards (*e.g.*, Ca), *i.e.*, the transition elements exhibit variable continuous fractionation during ablation in comparison relative to the internal standard (S.L. Jackson, pers. comm., 1995). Figure 3 of Fryer *et al.* (1995) illustrates the relative fractionation of the transition elements relative to lithophile elements commonly used as internal standards (*e.g.*, Ca or Si).

On the basis of the above discussion, we are not confident about the accuracy of the Ni value recommended for the STAG garnet by Fedorowich *et al.* (1995), as this garnet has only been analyzed by ICP–MS, and these results have not been corroborated by another technique (*e.g.*, INAA). Furthermore, we note that the Guelph micro-PIXE value of 69 ppm published by Fedorowich *et al.* (1995) was determined utilizing "Method A" (as outlined previously). Application of the now preferred "Method C" for the STAG garnet gives 65 ppm Ni with the standard deviation for 15 different spots being ±5 ppm. The Ni/Fe ratio in this case is 7, which corresponds closely to that of the GSR–5 glass (R = 6.5), where we observed the agreement between measured and nominal Ni concentrations to be within 3%. The measured value, 65 ppm, is approximately 10% higher than those reported for STAG garnet: 59 ± 1 ppm Ni (by LAM–ICP–MS), 56 ± 2 ppm Ni (by solution ICP–MS) and 57 ± 2 ppm Ni (micro-PIXE analysis conducted at the Commonwealth Scientific and Industrial Organization, CSIRO, Sydney, Australia), as reported by Fedorowich *et al.* (1995); see Figure 5. Details of the error estimates in the other measurements were not given. The difference between the Guelph and CSIRO PIXE results may be due to the two different software data-reduction schemes (Ryan *et al.* 1990, Maxwell *et al.* 1989, 1995) employed by the respective facilities. However, as shown in the present study, the Guelph micro-PIXE facility produces reliable Ni determinations over the range of concentrations 30–130 ppm that is of interest for mantle garnet. This tends to support our result of 65 ppm for the STAG garnet. As an independent test of accuracy, we were able to analyze a garnet megacryst (GHR–1) lent to us by Anglo American Research Laboratories (Pty), Johannesburg, South Africa; this had been characterized previously by instrumental neutron-activation analysis. One sample consisting of acid-leached grains gave a Ni result of 121 ppm, whereas a second sample consisting of unleached grains gave 117 ppm; the error estimate for these INAA results (1σ) is ±4%. The micro-PIXE value of 119.5 ± 4.5 ppm (mean over 15 spots) agrees closely with the INAA value of 120.5 ± 3.5 ppm, as shown in Figure 5. The merit of developing one or more well-characterized garnet standards is obvious.

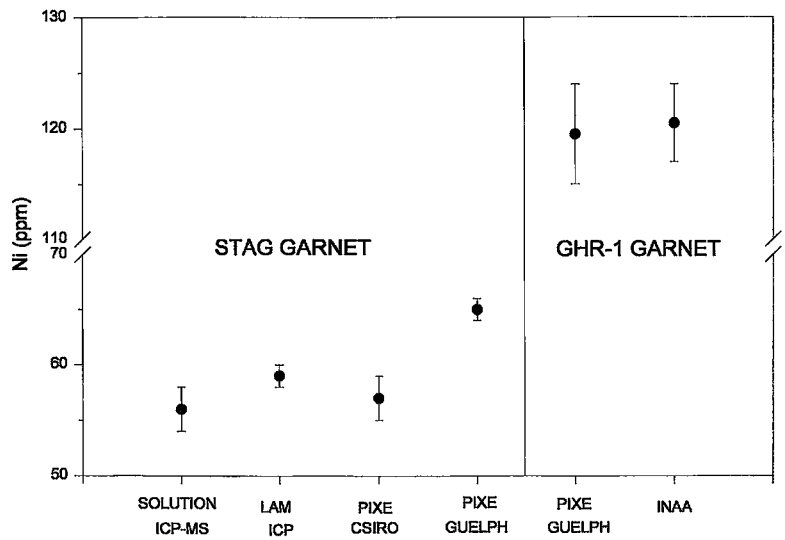

FIG. 5. Comparison of measured concentrations of Ni in STAG garnet and in GHR–1 megacryst.

Implications for thermometry

Single-spot analysis of a set of 100 mantle garnet grains is the common practice for the application of Ni thermometry in diamond-exploration programs. The Ni concentrations are usually converted to formation temperatures using the calibration established by Griffin *et. al.* (1989) and refined by Griffin & Ryan (1995); this is shown in Figure 6a. For a single-spot analysis (with 3–4 minute data-collection period)

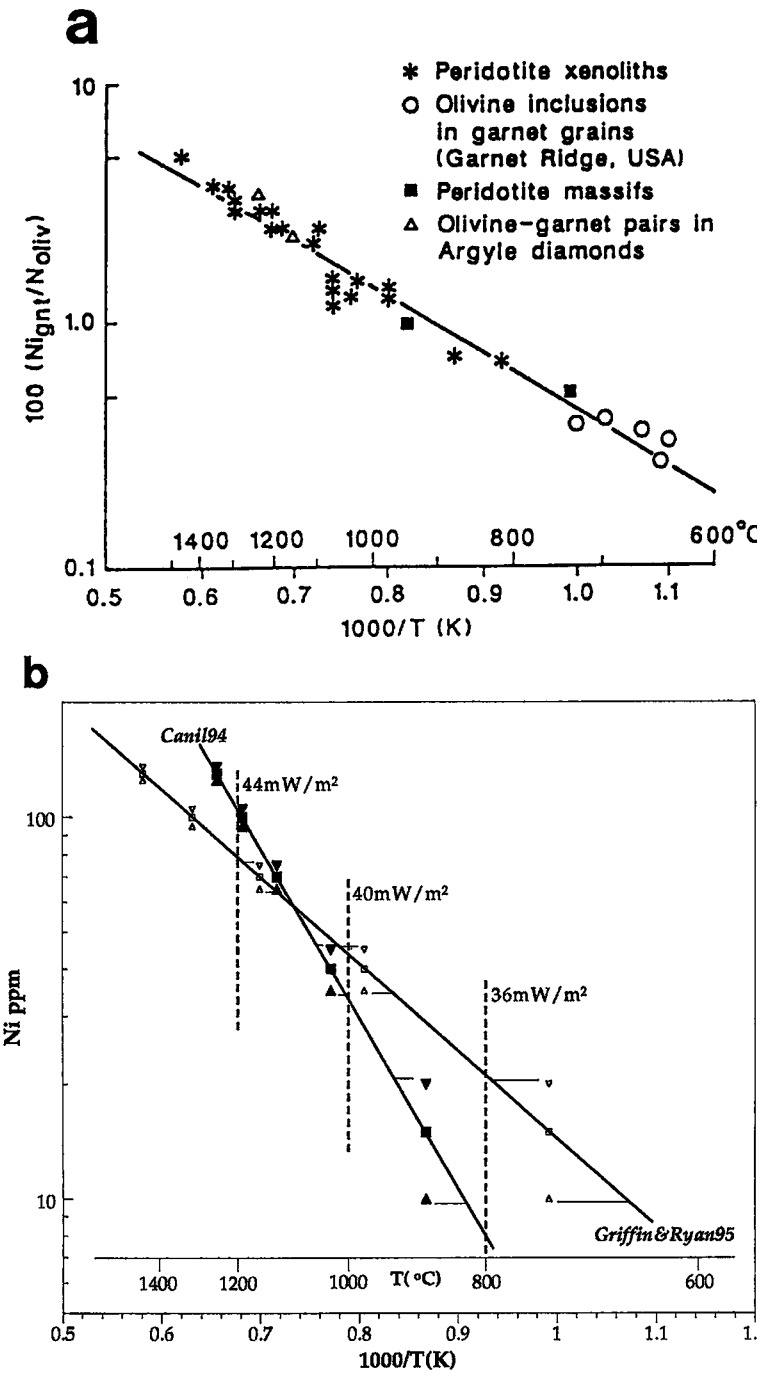

FIG. 6. (a) Ni concentration ratio (distribution coefficient) in coexisting garnet and olivine as a function of temperature (Griffin *et al.* 1989, Griffin and Ryan 1995). Reproduced by permission of C.G. Ryan and Elsevier Science Publishers. (b) Ni thermometer calibrations according to Griffin & Ryan (1995) and to Canil (1994). Estimates of measurement error shown are for a single 4-minute micro-PIXE measurement using the Guelph methodology. Temperature errors associated with typical analyses of Ni in mantle garnets at 15, 40, 70, 100 and 130 ppm concentration are illustrated for the calibration of Griffin & Ryan (1995) with open symbols and for that of Canil (1994) with filled symbols. Heavy dashed lines labeled 36 mW/m^2, 40 mW/m^2 and 44 mW/m^2 are the temperatures at which the graphite–diamond transition is intersected by the steady-state geotherm indicated. Garnet with "Ni temperatures" to the left of the known (or assumed) geotherm are interpreted to be derived from the stability field of diamond.

utilizing the Guelph methodology, associated statistical and fitting uncertainty in the determination of Ni concentration is in the 5–8 ppm range. The use of the top-hat filter causes this uncertainty to be somewhat larger than would be the case if a fitted continuum background were used. However, the standard deviation in concentrations measured for 10 or 15 spots is 4–6 ppm. If Ni is distributed homogeneously, which we believe to be the case, then the standard deviation should be equal to the fitting uncertainty. We deduce that the fitting uncertainty may be slightly overestimated, and we therefore adopt the standard deviation of the multispot measurement as the statistical uncertainty of a single measurement.

Thus single-spot analyses of garnet samples with Ni concentrations in the range 15–130 ppm have associated statistical uncertainties of approximately 5 ppm. Analysis of 100 grains of garnet to produce temperature–frequency stack histograms, as utilized in diamond-exploration programs (*e.g.*, Griffin & Ryan 1993) will, of course, tend to smooth any statistical errors in Ni determination. However, as noted by Kjarsgaard (1992), application of Ni concentration data requires a well-constrained calibration of the Ni thermometer. Figure 6b illustrates the consequences of a 5-ppm variation in Ni determination associated with a single spot analysis at the 15, 40, 70, 100 and 130 ppm Ni concentration level; the result is illustrated for both the published calibrations of the Ni thermometer, *i.e.*, those of Griffin & Ryan (1995) and of Canil (1994). In the concentration range of approximately 40–70 ppm, temperatures derived from the two calibrations differ by less than the uncertainty of a single-spot measurement. However, at lower and higher Ni content, the divergence of the two calibrations causes temperature differences that exceed the error of measurement. Further refinement of measurement uncertainty, therefore, appears less important than a resolution of the difference between the two published calibrations.

Acknowledgements

The work described was supported in part by the Natural Sciences and Engineering Research Council of Canada. We are grateful to A.R. Ramsden for supplying some of the now scarce GSD–50 and to J.H. Gilles Laflamme for preparing polished sections. We thank T.W. Sissons for preparing the BHVO–1, and G.K. Czamanske for repolishing and recoating it. Our thanks are due to G. Read at Anglo American Research Laboratories (Pty) Ltd, Johannesburg, South Africa, for permission to reproduce their Guelph micro-PIXE data for the GHR–1 garnet, and to R. Hart at the Schonland Centre, Johannesburg, for permission to reproduce his INAA data for this sample of garnet. The comments of the two reviewers and the editor are much appreciated.

References

Adam, J., Green, T.H. & Sie, S.H. (1993): Proton microprobe determined partitioning of Rb, Sr, Ba, Y, Zr, Nb and Ta between experimentally produced amphiboles and silicate melts with variable F content. *Chem. Geol.* **109**, 29-49.

Benjamin, T.M., Duffy, C.J. & Rogers, P.S.Z. (1988): Geochemical utilization of nuclear microprobes. *Nucl. Instrum. Methods Phys. Res.* **B30**, 454-458.

Campbell, J.L., Higuchi, D., Maxwell, J.A. & Teesdale, W.J. (1993): Quantitative PIXE microanalysis of thick specimens. *Nucl. Instr. Methods Phys. Res.* **B77**, 95-109.

_____, Maxwell, J.A., Teesdale, W.J., Wang, J.-X. & Cabri, L.J. (1989): Micro-PIXE as a complement to electron probe microanalysis in mineralogy. *Nucl. Instrum. Methods Phys. Res.* **B44**, 347-356.

Canil, D. (1994): An experimental calibration of the "Nickel in Garnet" geothermometer with applications. *Contrib. Mineral. Petrol.* **117**, 410-420.

Czamanske, G.K., Sisson, T.W., Campbell, J.L. & Teesdale, W.J. (1993): Micro-PIXE analysis of silicate reference standards. *Am. Mineral.* **78**, 893-903.

Ewart, A. & Griffin, W.L. (1994): Application of proton microprobe data to trace element partitioning in volcanic rocks. *Chem. Geol.* **117**, 251-284.

Fedorowich, J.S., Jain, J.C., Kerrich, R. & Sopuck, V. (1995): Trace element analysis of garnet by laser-ablation microprobe ICP–MS. *Can. Mineral.* **33**, 469-480.

Foley, S.F. & van der Laan, S.R. (1994): Preface. *In* Trace element partitioning with Application to magmatic Processes (S.F. Foley & S.R. van der Laan, S.R., eds.). *Chem. Geol. (Spec. Issue)* **117**, vii-xiv.

Fryer, B.J. Jackson, S.E. & Longerich, H.P. (1995): The design, operation and role of the laser-ablation microprobe coupled with an inductively coupled plasma – mass spectrometer (LAM–ICP–MS) in the earth sciences. *Can. Mineral.* **33**, 303-312.

Gladney, E.S. & Roelandts, I. (1988): 1987 compilation of elemental concentration data for USGS BHVO–1, MAG–1, QLO–1, RGM–1, SCo–1, SDC–1, SGR–1, and STM–1. *Geostandards Newsletter* **12**, 253-362.

_____ & _____ (1990): 1988 compilation of elemental concentration data for USGS geochemical exploration reference materials GXR–1 to GXR–6. *Geostandards Newsletter* **14**, 21-118.

Govindaraju, K. (1989): 1989 compilation of working values and sample description for 272 geostandards. *Geostandards Newsletter* **13** (*special issue*), 1-113.

Green, T.H. (1994): Experimental studies of trace-element partitioning applicable to igneous petrogenesis – Sedona 16 years later. *Chem. Geol.* **117**, 1-36.

GRIFFIN, W.L., COUSENS, D.R., RYAN, C.G., SIE, S.H. & SUTER, G.F. (1989): Ni in chrome pyrope garnets: a new geothermometer. *Contrib. Mineral. Petrol.* **103**, 199-202.

_____ & RYAN, C.G. (1993): Trace elements in garnets and chromites: evaluation of diamond exploration targets. *In* Diamonds: Exploration, Sampling and Evaluation (P.A. Sheahan & A. Chater, eds.). Short Course Proc., Prospectors and Developers Association of Canada, Toronto, Ontario (187-211).

_____ & _____ (1995): Trace elements in indicator minerals: area selection and target evaluation in diamond exploration. *J. Geochem. Explor.* **53**, 311-337.

HALDEN, N.M., CAMPBELL, J.L. & TEESDALE, W.J. (1995): PIXE analysis in mineralogy and geochemistry. *Can. Mineral.* **33**, 293-302.

HERVIG, R.L., SMITH, J.V. & DAWSON, J.B. (1986): Lherzolite xenoliths in kimberlite and basalts: petrogenetic and crystallochemical significance of some minor and trace elements in olivines, pyroxene, garnet and spinel. *Trans. Roy. Soc. Edinburgh, Earth Sci.* **77**, 181-201.

JACKSON, S.E., LONGERICH, H.P., DUNNING, G.R. & FRYER, B.J. (1992): The application of laser-ablation microprobe – inductively coupled plasma – mass spectrometer (LAM–ICP–MS) to *in situ* trace-element determinations in minerals. *Can. Mineral.* **30**, 1049-1064.

JEFFRIES, T.E., PERKINS, W.T. & PEARCE, N.J.G. (1995): Comparison of infrared and ultraviolet laser probe microanalysis inductively coupled plasma mass spectrometry in mineral analysis. *Analyst* **120**(4), 1365-1372.

KJARSGAARD, B.A. (1992): Is Ni in chrome pyrope garnet a valid diamond exploration tool? *Geol. Surv. Can., Pap.* **92-1E**, 315-322.

LARSSON, N.P.-O., TAPPER, U.A.S. & MARTINSSON, B.G. (1989): Characterization of the response function of a Si(Li) detector using an absorber technique. *Nucl. Instrum. Methods Phys. Res.* **B43**, 574-580.

LUDDEN, J.N., FENG, RUI, GAUTHIER, G., STIX, J., LANG, SHI, FRANCIS, D., MACHADO, N. & WU, GUOPING (1995): Application of LAM–ICP–MS analysis to minerals. *Can. Mineral.* **33**, 419-434.

MAXWELL, J.A., CAMPBELL, J.L. & TEESDALE, W.J. (1989): The Guelph PIXE software package. *Nucl. Instrum. Methods Phys. Res.* **B43**, 218-230.

_____, TEESDALE, W.J. & CAMPBELL, J.L. (1994): Compensation schemes for peak-tailing uncertainties in PIXE spectra, using the GUPIX code. *Nucl. Instrum. Methods Phys. Res.* **B94**, 172-179.

_____, _____ & _____ (1995): The Guelph PIXE software package II. *Nucl. Instrum. Methods Phys. Res.* **B95**, 407-421.

MCCARTHY, J.J. & SCHAMBER, F.H. (1981): Least-squares fit with digital filter. *Nat. Bur. Standards, Spec. Publ.* **604**.

MERLET, C. & BOUDINIER, J.-L. (1990): Electron microprobe determination of minor and trace transition elements in silicate minerals: a new method and its application to mineral zoning in the peridotite nodule PHN1611. *Chem. Geol.* **83**, 55-69.

MOORE, R.O., GRIFFIN, W.L., GURNEY, J.J., RYAN, C.G., COUSENS, D.R. SIE, S.H. & SUTER, G.F. (1992): Trace element geochemistry of ilmenite megacrysts from the Monastery kimberlite, South Africa. *Lithos* **29**, 1-18.

MYERS, A.T., HAVENS, R.G., CONNOR, J.J., CONKLIN, N.M. & ROSE, H.J., JR. (1976): Glass reference standards for the trace element analysis of geological materials – compilation of inter-laboratory data. *U.S. Geol. Surv., Prof. Pap.* **1013**.

PERKINS, W.T., PEARCE, N.J.G. & JEFFRIES, T.E. (1993): Laser ablation inductively coupled plasma mass spectrometry: a new technique for the determination of trace and ultra-trace elements in silicates. *Geochim. Cosmochim. Acta* **57**, 475-482.

REED, S.J.B. (1990): Recent developments in geochemical microanalysis. *Chem. Geol.* **83**, 1-9.

RYAN, C.G., COUSENS, D.R., SIE, S.H., GRIFFIN, W.L., SUTER, G.F. & CLAYTON, E. (1990): Quantitative PIXE microanalysis of geological material using the CSIRO proton microprobe. *Nucl. Instrum. Methods Phys. Res.* **B47**, 55-71.

SHIMIZU, N. & ALLÈGRE, C.S. (1978): Geochemistry of transition elements in garnet lherzolite nodules in kimberlites. *Contrib. Mineral. Petrol.* **47**, 41-50.

STIMAC, J. & HICKMOTT, D. (1994): Trace element partition coefficients for ilmenite, orthopyroxene and pyrrhotite in rhyolite determined by micro-PIXE analysis. *Chem. Geol.* **117**, 313-330.

SWEENEY, R.J., GREEN, D.H. & SIE, S.H. (1992): Trace and minor element partitioning between garnet and amphibole and carbonatitic melt. *Earth Planet. Sci. Lett.* **113**, 1-14.

VICENZI, E., GREEN, T.H. & SIE, S.H. (1994): Effect of oxygen fugacity on trace-element partitioning between immiscible silicate melts at atmospheric pressure: a proton and electron microprobe study. *Chem. Geol.* **117**, 355-360.

XIE XUEJING, YAN MINGCAI, WANG CHUNSHU, LI LIANZHONG & SHEN HUIJUN (1989): Geochemical standard reference samples GSD 9–12, GSS 1–8, and GSR 1–6. *Geostandards Newsletter* **13**, 83-179.

Received March 1, 1995, revised manuscript accepted September 28, 1995.